

## **Supporting Information For**

### **HIV-1 Capsid Function is Regulated by Dynamics: Quantitative Atomic-Resolution Insights by Integrating Magic-Angle-Spinning NMR, QM/MM, and MD**

Huilan Zhang<sup>1,2,#</sup>, Guangjin Hou<sup>1,2,#</sup>, Manman Lu<sup>1,2</sup>, Jinwoo Ahn<sup>2,3</sup>, In-Ja L. Byeon<sup>2,3</sup>, Christopher J. Langmead<sup>4</sup>, Juan R. Perilla<sup>5</sup>, Ivan Hung<sup>6</sup>, Peter L. Gor'kov<sup>6</sup>, Zhehong Gan<sup>6</sup>, William W. Brey<sup>6</sup>, David A. Case<sup>7</sup>, Klaus Schulten<sup>5</sup>, Angela M. Gronenborn<sup>2,3\*</sup>, and Tatyana Polenova<sup>1,2\*</sup>

<sup>1</sup>Department of Chemistry and Biochemistry, University of Delaware, Newark, Delaware 19716, United States; <sup>2</sup>Pittsburgh Center for HIV Protein Interactions, University of Pittsburgh School of Medicine, 1051 Biomedical Science Tower 3, 3501 Fifth Ave., Pittsburgh, PA 15261, United States; <sup>3</sup>Department of Structural Biology, University of Pittsburgh School of Medicine, 3501 Fifth Ave., Pittsburgh, PA 15261, United States; <sup>4</sup>Computer Science Department, Carnegie Mellon University, Gates Hillman Center, 5000 Forbes Avenue, Pittsburgh, PA, United States; ; <sup>5</sup>Department of Physics and Beckman Institute for Advanced Science and Technology University of Illinois at Urbana-Champaign, Urbana, Illinois 61801; <sup>6</sup>National High Magnetic Field Laboratory, Florida State University, Tallahassee, FL, 32310, United States; <sup>7</sup>Department of Chemistry and Chemical Biology, Rutgers University, 174 Frelinghuysen Road, Piscataway, NJ 08854-8087, United States

<sup>#</sup>These authors have contributed equally

**\*Corresponding authors:** Tatyana Polenova, Department of Chemistry and Biochemistry, University of Delaware, Newark, DE, USA, Tel.: (302) 831-1968; Email: tpolenov@udel.edu; Angela M. Gronenborn, Department of Structural Biology, University of Pittsburgh School of Medicine, 3501 Fifth Ave., Pittsburgh, PA 15260, USA, Tel.: (412) 648-9959; Email: amg100@pitt.edu

**Classification:** Biological Sciences- Biophysics and Computational Biology

**Keywords:** magic-angle spinning NMR, HIV-1 capsid, CA protein assemblies, HIV-AIDS, conformational dynamics, chemical shift anisotropy, quantum mechanics/molecular mechanics

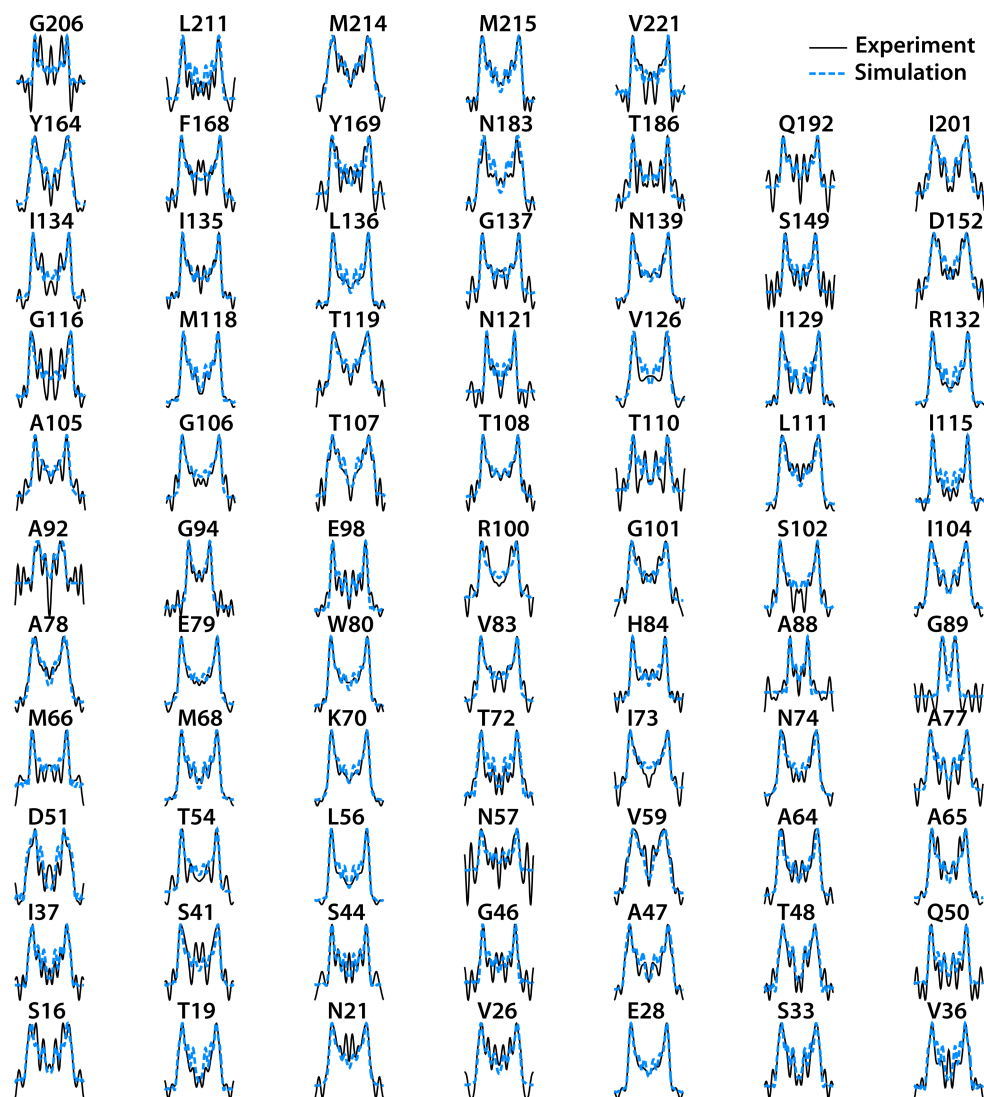


**Figure S1.** Experimental (solid black lines) and simulated (dashed blue lines)  $^{15}\text{N}$  CSA lineshapes for different residues in tubular assemblies of CA HXB2 extracted from the  $\text{R8}_1^3$ -RNCSA 3D spectra, recorded at the magnetic field of 21.1 T and the MAS frequency of 14 kHz.

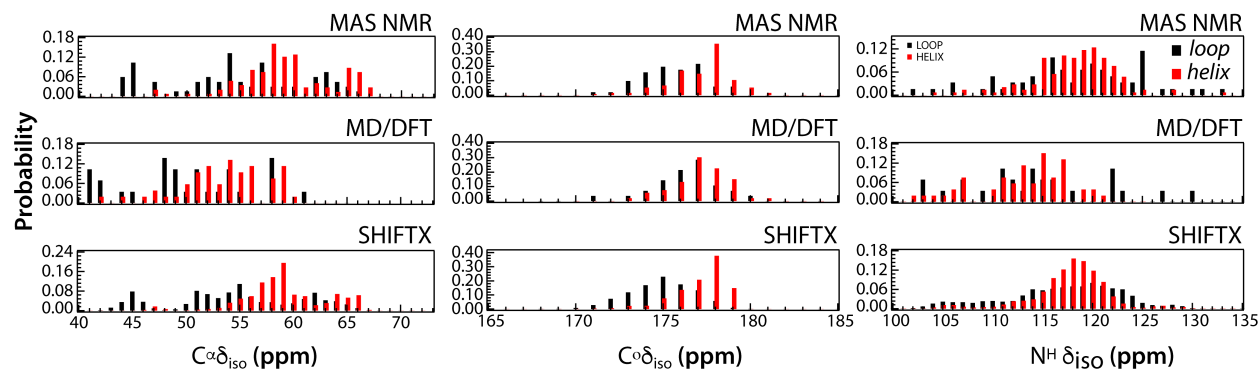


**Figure S2.** Distribution plots for the isotropic  $^{13}\text{C}^\alpha$  (left),  $^{13}\text{C}^\beta$  (middle), and  $^{15}\text{N}^{\text{H}}$  (right) chemical shifts in HIV-1 CA assemblies. Top: experimental MAS NMR; middle, calculated from MD/DFT; bottom, calculated by SHIFTX as the averaged values over the MD trajectory. The distributions for helical regions are shown in red, for loops- in black.

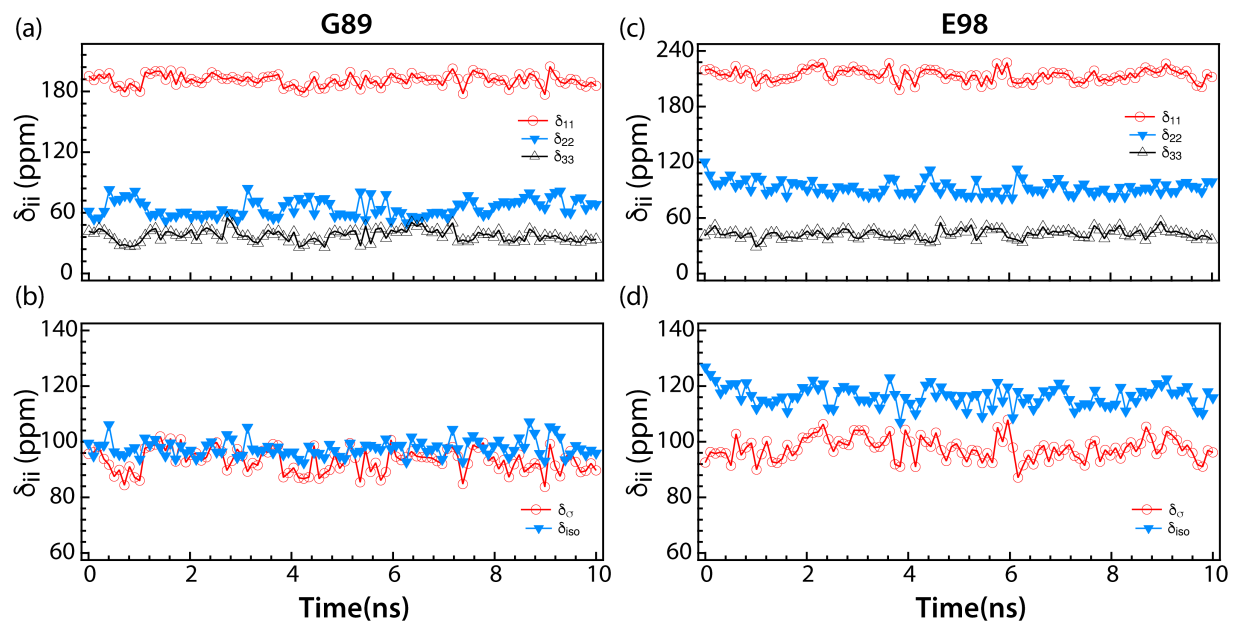


**Figure S3.** Principal components of  $^{15}\text{N}$  CSA tensor,  $\delta_{ii}$ ,  $\delta_{\sigma}$ , and  $\delta_{\text{iso}}$ , calculated along the MD trajectory, for selected CA residues: G89 (a, c) and E98 (b, d). For the calculations, 100 frames were used from the first 10 ns of the 100-ns MD trajectory.

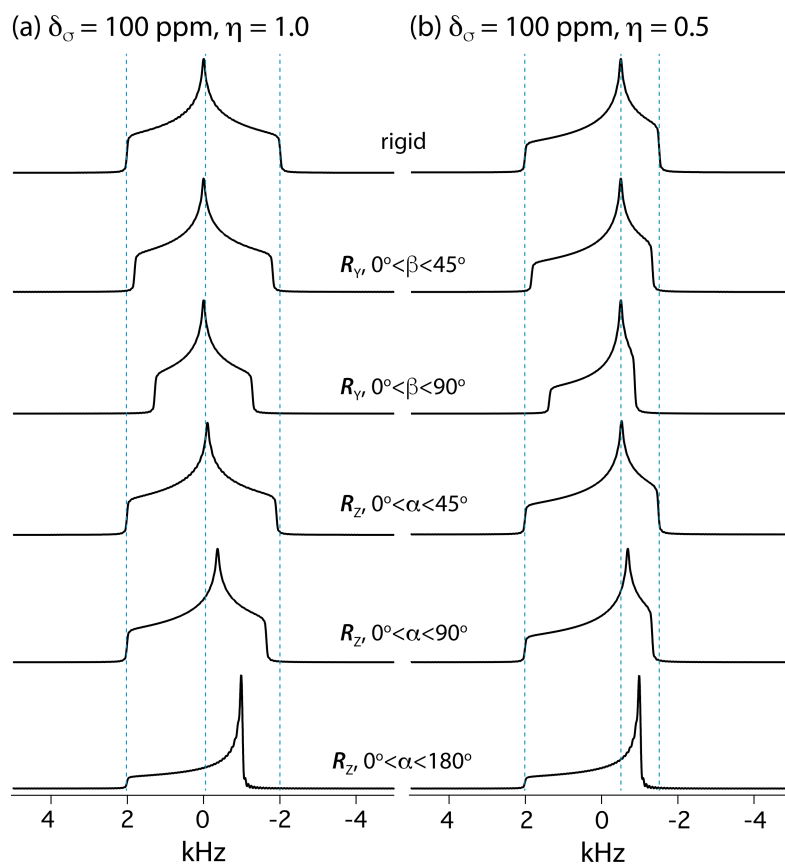


**Figure S4.** Simulated rigid and motionally reduced  $^{15}\text{N}$  CSA line shapes for the sites with the following CSA NMR parameters: (a)  $\delta_\sigma = 100$  ppm and  $\eta = 1.0$ ; (b)  $\delta_\sigma = 100$  ppm and  $\eta = 0.5$ . The Euler angles are indicated next to each line shape.

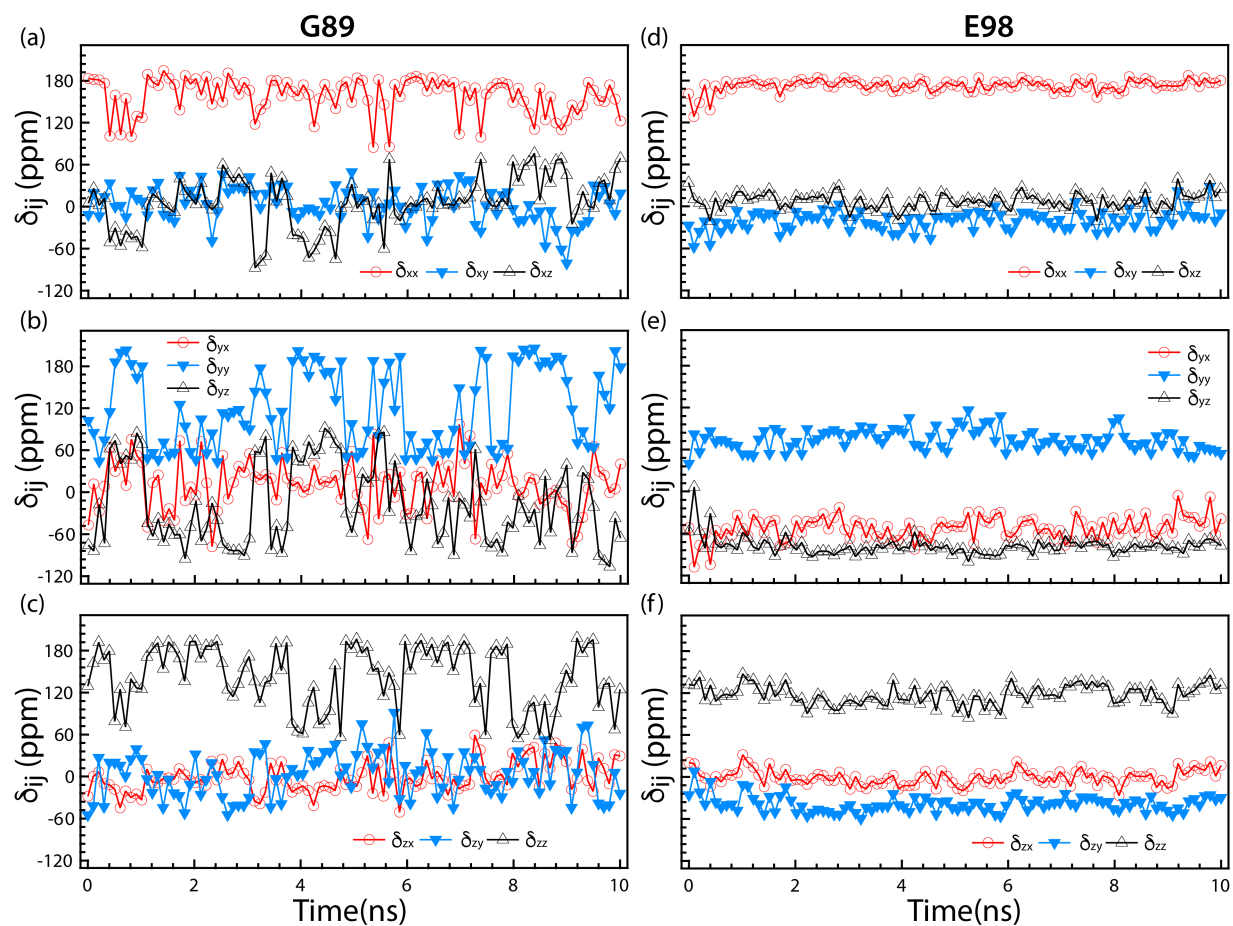


**Figure S5.** Individual components of  $^{15}\text{N}$  CSA tensor  $\delta_{ij}$  (molecular fixed frame representation), calculated along the MD trajectory, for selected CA residues: G89 (a-c) and E98 (d-f). For the calculations, 100 frames were used from the first 10 ns of the 100-ns MD trajectory.

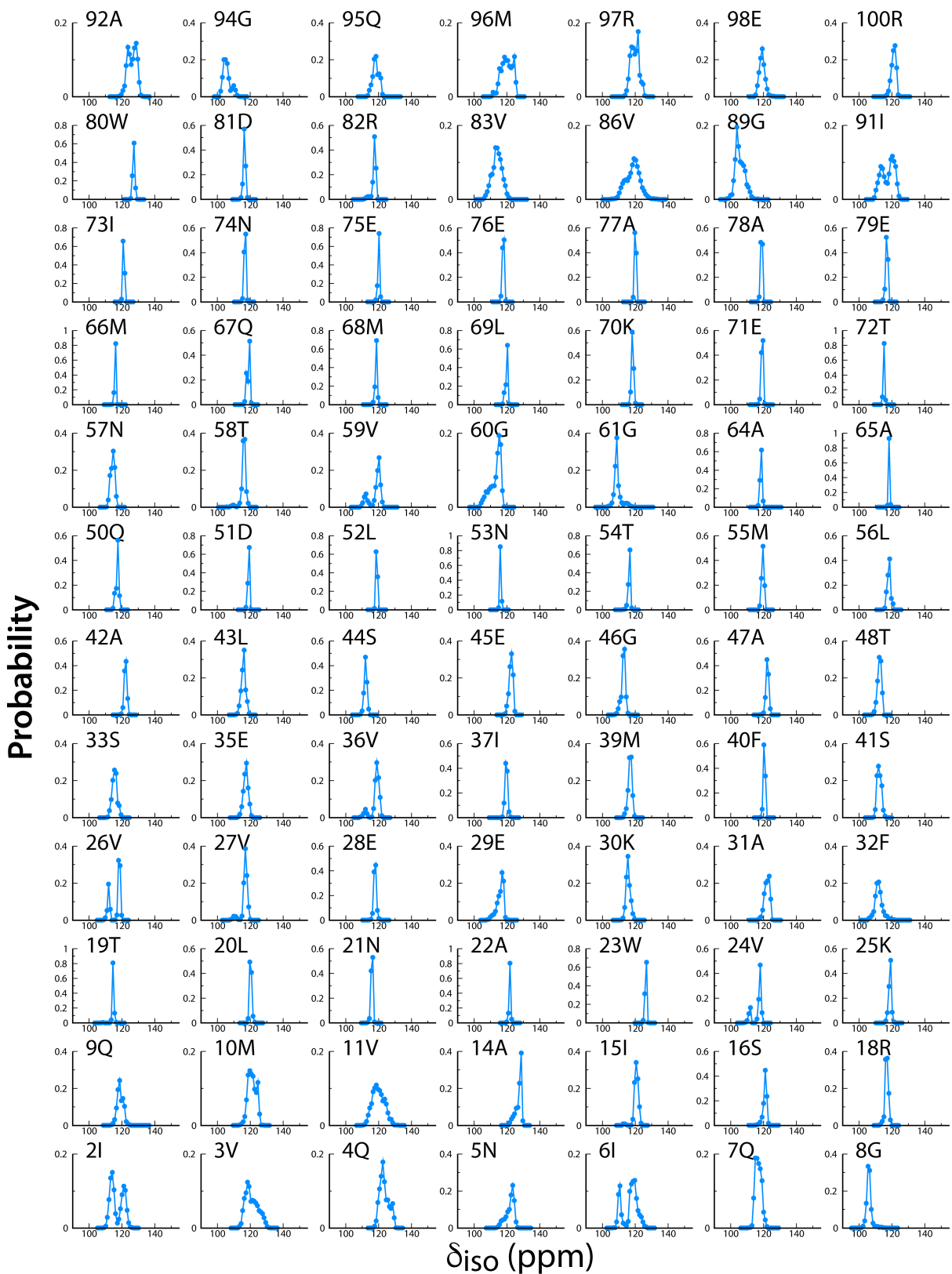


**Figure S6.** Probability distributions of  $^{15}\text{N}$  isotropic chemical shifts of HIV-1 CA calculated by Shiftx based on 5000 frames extracted from 100 ns MD simulation.

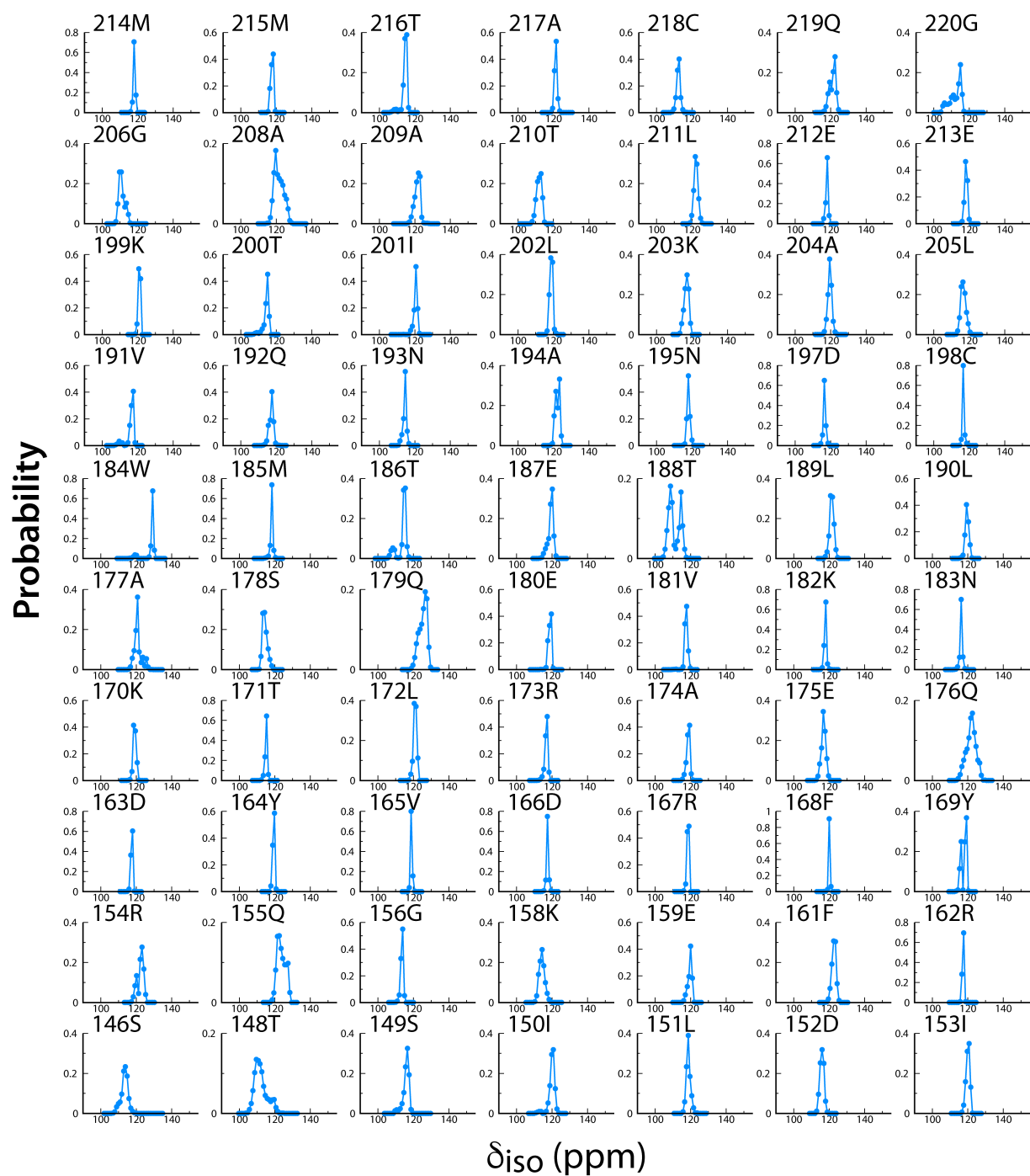


**Figure S6.** (con'd) Probability distributions of  $^{15}\text{N}$  isotropic chemical shifts of HIV-1 CA calculated by Shiftx based on 5000 frames extracted from 100 ns MD simulation.



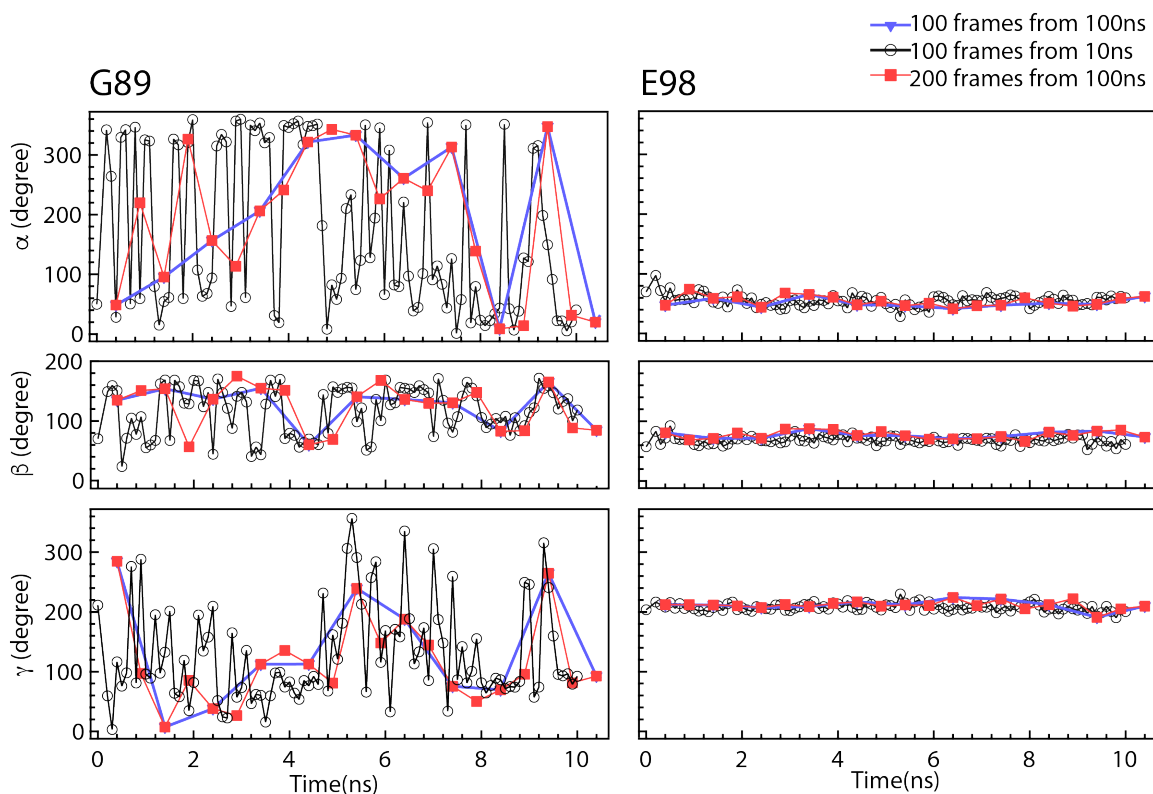


**Figure S7.** Euler angles of the  $^{15}\text{N}$  CSA tensors for G89 and E98 residues of CA, calculated by MD/DFT with different sampling schedules: 200 frames from 100-ns MD trajectory, red; 100 frames from 100-ns MD trajectory, blue; 100 frames from the first 10 ns of the 100-ns MD trajectory, black. The corresponding  $^{15}\text{N}$  CSA parameters for G89 are:  $\delta_\sigma = 28.92$  ppm,  $\eta_\sigma = 0.11$ ;  $\delta_\sigma = 23.28$  ppm,  $\eta_\sigma = 0.10$ ;  $\delta_\sigma = 23.75$  ppm,  $\eta_\sigma = 0.12$ . The corresponding  $^{15}\text{N}$  CSA parameters for E98 are:  $\delta_\sigma = 93.83$  ppm,  $\eta_\sigma = 0.52$ ;  $\delta_\sigma = 93.00$  ppm,  $\eta_\sigma = 0.53$ ;  $\delta_\sigma = 92.94$  ppm,  $\eta_\sigma = 0.54$ .

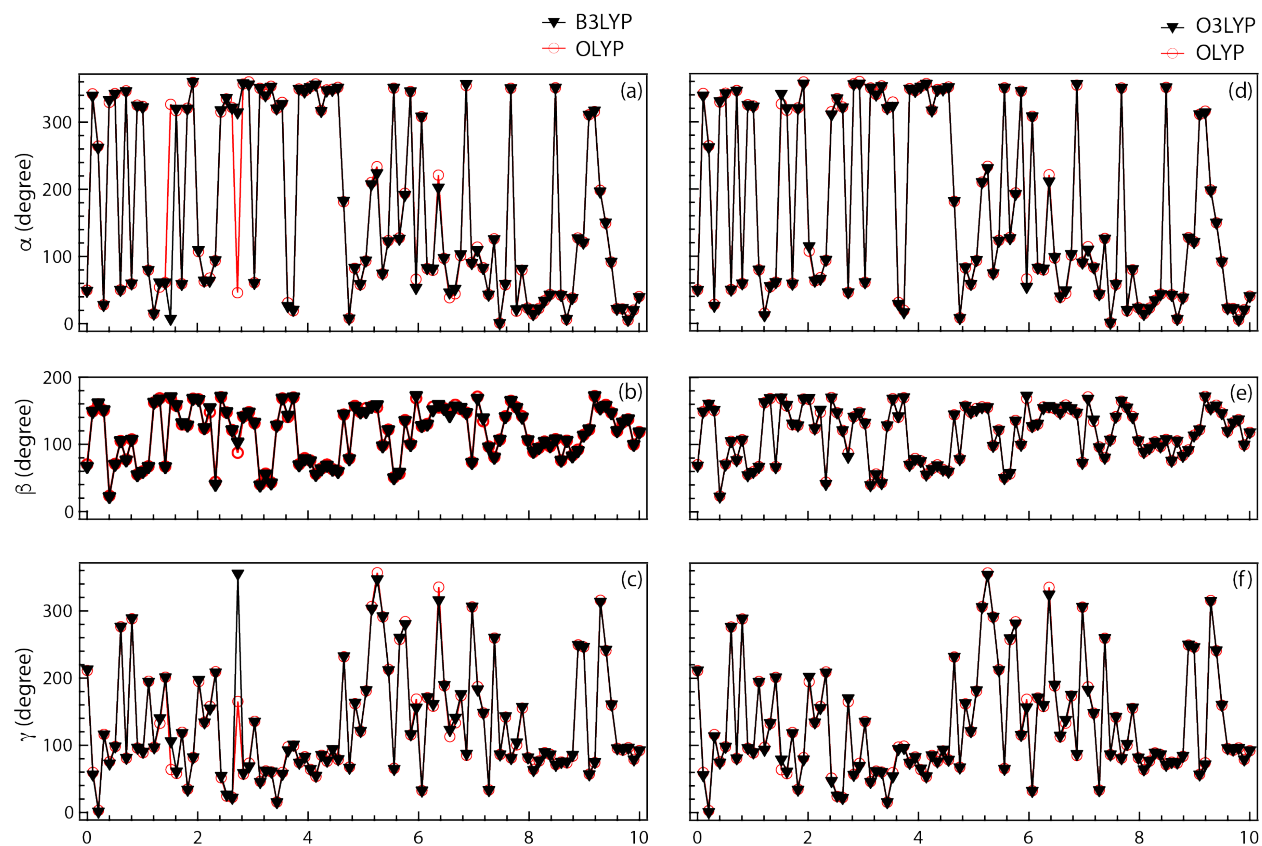


**Figure S8.** Euler angles of the  $^{15}\text{N}$  CSA tensors for G89 residue in the molecular frame along the MD trajectory, calculated using (a-c) B3LYP and OLYP functionals (black and red symbols, respectively), and (d-f) O3LYP and OLYP functionals (black and red symbols, respectively). The angles were calculated using  $\delta_\sigma = 25.63$ , 23.75, and 24.66 ppm for B3LYP, OLYP, and O3LYP, respectively. Note that the differences are small for  $\delta_\sigma$  computed with the three functionals. For the calculations, 100 frames were used from the first 10 ns of the 100-ns MD trajectory.